Stabilities and Electronic Properties of Two-Dimensional C_{36} Crystals

Shixuan Du, Yuanhe Huang,* Yuxue Li, and Ruozhuang Liu

Department of Chemistry, Beijing Normal University, Beijing, 100875, China

Received: September 26, 2001; In Final Form: February 15, 2002

The structure and electronic properties for five two-dimensional (2D) C_{36} slabs with a C_{36} per unit cell and the supergraphite structure with two C_{36} per unit cell are calculated using ab initio self-consistent field crystal orbital method based on B3LYP density functional theory. The calculations show that the structure stabilities are dependent on steric hindrance and size of aromatic domains. All the models are semiconductors. The band structures of corresponding anionic C_{36}^{m-} ($m = 1-4$) slabs with a C_{36} per unit cell are also calculated. It is found that the extra electrons fill the unoccupied bands of neutral crystals almost in a rigid-band manner. The superconducting possibility in those metallic slabs is discussed on the basis of the electron−phonon coupling mechanism. It seems that the 2D C_{36} slabs with a C_{36} cage per unit cell cannot produce a superconducting transition temperature much higher than those in alkali metal-doped C_{60} crystals.

1. Introduction

Recently, a C_{36} solid has attracted great interest due to its special structure. Unlike large fullerenes, C_{36} has high curvature and increased strain energy owing to adjacent pentagon rings,[1] hence, strong intermolecular bonds can be formed between neighbor C_{36} cages.[1−4] It has been pointed out that C_{36} can be a building block for oligomers, polymers, and solids.[5−8] Theoretical calculations had predicted that the three-dimensional (3D) rhombohedral C_{36}-fullerenes could produce high superconducting transition temperature (T_c)[2] and the 1D C_{36} polymers are semiconductors.[9] How about the two-dimensional (2D) C_{36} slabs? Are their properties similar to 1D or 3D cases from the view of theoretical calculations? Several 2D C_{36} slabs have been supposed,[5,6,8,10] most of them have more than one C_{36} cage per unit cell.[5,6,10] For those with one C_{36} per unit cell, there are no detail discussions. Here we study five 2D C_{36} models with one C_{36} per unit cell, their energies and electronic structures are calculated using ab initio self-consistent-field crystal orbital (SCF−CO) method. We also calculated the supergraphite structure [5] with two C_{36} cages per unit cell for better understanding possible 2D C_{36} structures and properties. Stability related to the geometrical structure is discussed, and the electronic properties are compared with those of 1D and 3D structures. As a matter of fact, some of the slabs studied here can be built from the extension of the 1D C_{36} models.[9] Hence we can also explore the influence on the electronic properties due to interchain interaction. Furthermore, considering the increase of electrical conductivity upon doping with alkali metals[1] and higher superconducting possibility of anionic C_{36},[11] C_{36}^{m-} ($m = 1-4$) slabs were also calculated and the change of electronic properties with m are investigated. Possibility of superconductivity is discussed on the basis of the electron−phonon (e−p) coupling mechanism for 2D C_{36} polymers at the same time. We would like to point out that low dimensional C_{36} crystals have not been obtained so far, but possibly similar to the case in the development of C_{60},[12] they can be discovered soon. Therefore, prior theoretical studies are useful to examine their possible structures and electronic properties.

* Author to whom correspondence should be addressed.

2. Models and Methods

The experimental evidence and a recent study of hydrogenated C_{36} favor D_{6h} 36:15 isomer,[1,13,14] though several theoretical calculations indicated that isomer 36:14 is essentially isoenergetic with or more stable than 36:15.[5,15,16] Therefore, we focus only on those with higher symmetries (shown in Figure 1), though there are many possible isomers of C_{36} slabs. The five 2D slabs A−E in Figure 1 can all be built from isomer 36:15 with different linking patterns, and each unit cell contains one C_{36} cage. It has been considered that the relaxation of C_{36} cages due to the forming of intermolecular bonds between neighbor C_{36} molecules. The symmetries of C_{36} units are D_{6h} for A and D_{2h} for B, C, D, and E, respectively. According to our knowledge, these models have not been calculated except slab E. Though slab E may have D_{6h} symmetry, we obtained a more stable D_{2h} structure that deviates from D_{6h} a little. The geometrical parameters of C_{36} cages in slabs B and C were obtained from the full optimization results of planar C_{36} quintumers, while those in slabs A, D, E, and supergraphite were obtained from heptamers and tetramer, respectively, with Gaussian 98 program package.[17] Because these oligomers are quite big, the ONIOM technique implemented in Gaussian 98 was used when optimizing the geometry.[18,19] The quintumers, heptamers, or tetramer were divided into two layers, the central C_{36} cages used for the unit cell in SCF−CO calculations were calculated using hybrid Hartree−Fock/density-functional-theory (HF/DFT) molecular method of B3LYP[20,21] with 3-21G basis set,[22] while the others using semiempirical MNDO approach.[23]

For the calculation of band structures of the C_{36} slabs, we use ab initio SCF−CO methods with B3LYP/3-21G in CRYSTAL 98 program.[24] Intermolecular bonds are allowed to further relax through the point-wise optimization, i.e., optimizing the length of translation vectors a and b, but other geometrical parameters are kept unchanged. In SCF−CO calculations, shrinking factors are set to 20, default values of convergence criteria in CRYSTAL 98 program are used. The optimized intermolecular bonds and translation lengths are also given in Figure 1. Band structures of C_{36}^{m-} ($m = 1-4$) slabs with a C_{36}

10.1021/jp013623n CCC: $22.00
Published on Web 03/20/2002

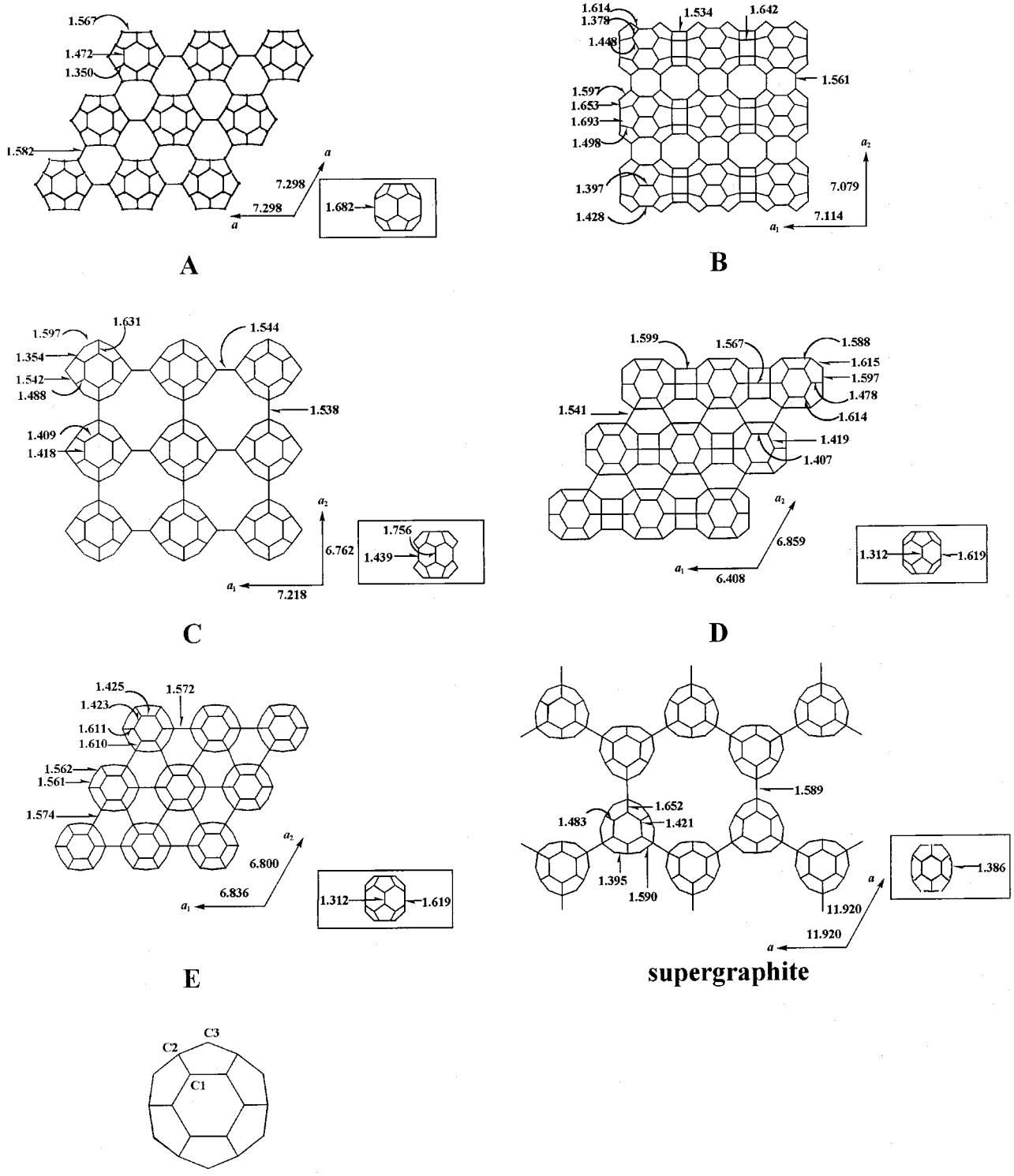

Figure 1. Models of C_{36} slabs (length unit: Å).

cage per unit cell are calculated using the same basis sets and the same geometrical structures of corresponding neutral slabs. Until now, no calculations have been given for the anionic polymers studied. Because the unit cell of a periodic system must be neutral, the charges are compensated by adding a uniform background charge density in CRYSTAL 98 program[24] for the calculation of charged systems. For a comparison, B3LYP/6-31G*[25] calculations have also been carried out without further geometric structure optimization for slabs A−E and the neutral supergraphite.

3. Results and Discussion

3.1. Structures and Stabilities. As shown in Figure 1, each C_{36} cage has 12, 16, 8, 20, and 12 linking bonds with neighbors for slabs A−E, respectively. The optimized intermolecular bond lengths are in the range of 1.534−1.642 Å, indicating that the five models are covalent 2D polymers. The translation lengths of these 2D C_{36} models are 6.408−7.298 Å, some longer than 6.68 Å suggested by electron-diffraction patterns except that of slab D along *a* direction.[1]

TABLE 1: Energies per C_{36} Cage Related to Neutral D_{6h} 36:15 Isomer (in eV)

	slab A		slab B		slab C		slab D		slab E	
basis set	3-21G	6-31G*	3-21G	6-31G*	3-21G	6-31G*	3-21G	6-31G*	3-21G	6-31G*
$m = 0$	3.59	4.50	−1.67	−0.12	−1.29	0.042	0.62	3.59	−1.58	1.48
$m = 1$	−3.47	−2.52	−7.10	−5.24	−8.02	−6.52	−5.45	−2.37	−7.54	−4.35
$m = 2$	−16.35	−15.35	−17.19	−15.23	−20.50	−18.96	−19.37	−16.64	−20.65	−17.56
$m = 3$	−33.84	−32.99	−31.57	−29.71	−37.60	−36.29	−41.69	−39.08	−41.22	−38.34
$m = 4$	−57.96	−57.22	−51.40	−47.96	−61.09	−60.38	−71.91	−69.99	−69.01	−66.88

The energies related to single isomer 36:15 molecule per C_{36} cage (ΔE) are listed in Table 1. Smaller ΔE means more stable. According to the values of Table 1, the order of stability for neutral slabs is B > E > C > D > A calculated with 3-21G, but B > C > E > D > A for the 6-31G* calculations. Though slab E is 0.29 eV more stable than slab C for the 3-21G calculations, it is 1.44 eV more unstable than slab C for the 6-31G* calculations. It can be found that stabilities have something to do with the number of the nearest neighbor C_{36} cages. Slabs B and C with less nearest neighbor C_{36} cages are more stable than the other three slabs by the 6-31G* results. Hence, steric hindrance possibly plays an important role in the stability of C_{36} crystals from a view of thermodynamics. Another important factor may be the aromatic degree of the C_{36} cages. It had been pointed out that the stability of fullerene derivative was increased by maximizing conventional aromatic domains.[26] Since a C_{36} cage has two naphthalenoid domains in slab B, but two benzenoid domains in slab C, therefore slab B is more stable than slab C. For the other three slabs, conventional aromatic domain is also the benzene rings. As to slab A, the bond length of hexagonal rings is 1.472 Å and deviates some big from 1.39 Å of benzene,[27] resulting in a decrease of conjugated degree. Besides, the shared sides of fused pentagons become 1.35 Å. It can be considered that double bonds are introduced into the five-membered rings, leading to a more unstable structure. Hence, slab A is less stable than slabs D and E. The distortion degree of C_{36} cage in slab D is bigger than that in slab E, which may bring larger strains, hence slab E is more stable than slab D. However, we cannot conclude that forming B and C is easier than others, since the experimental isomeric structure does not depend on its absolute thermodynamic stability.

Consider the supergraphite structure with two C_{36} cages per unit cell shown also in Figure 1. The number of the nearest neighbor C_{36} cages in this structure is three only. In addition, there are five benzenoid domains: two are in the polar region and three on the equatorial belt with C−C bond length about 1.39 Å, almost the same as that of benzene. Therefore, from the above discussion, the supergraphite should be the most stable structure among the polymers studied due to less steric hindrance and larger conventional aromatic domains. It is confirmed by our calculations. The ΔE is about 1.3 eV smaller than that of slab B for both 3-21G and 6-31G*. Our calculations show that the formation of the supergraphite and slab B can lead to the decrease of the whole system energy for both 3-21G and 6-31G* calculations.

For charged slabs, stability order is changed. Since structure relaxation is not considered, the change of stability is due mainly to the change of electronic energies. Calculation shows that the charges are mainly distributed on the hexacene belts for neutral slabs. When extra electrons are introduced, the charges on bonding atoms change little, the main changes occur on those atoms not participating in forming intermolecular bonds, such as nonbonding C2 and C3 atoms for slab B, or C1 atoms for A, C, D, and E.

3.2. Band Structures and Electronic Properties. The calculated 3-21G band structures and density of states (DOS) of neutral slabs are shown only in Figure 2, since 6-31G* band structures are similar to those with 3-21G in essence.

It can be seen that there exist energy gaps (E_g) between the highest occupied band (HOB) and the lowest unoccupied band (LUB) for slabs A−E. Their electronic properties obtained by both 3-21G and 6-31G* calculations are all listed in Table 2. Table 2 shows that these covalent 2D polymers are all semiconductors with the energy gaps of 0.58−3.97 eV. Compared with the 3-21G results, although the 6-31G* calculations give smaller E_g and higher top of HOB and bottom of LUB for all neutral semiconductive slabs, the electronic properties are no essential difference for both basis sets. A bigger E_g would be against the increase of reaction activity, since it is not favorable to electron excitation. Hence slab B with bigger E_g is possibly the stable structure, not only from a view of thermodynamics but also from dynamics. The calculated result of slab E is similar to that of the plane-wave pseudopotential LDA calculation,[8] indicating that slab E is a semiconductor. The LDA gave an E_g of 1.09 eV for slab E, being smaller than that obtained here. For the supergraphite, its band structures and DOS calculated at both 3-21G and 6-31G* levels are shown in Figure 3. It is calculated to be a semiconductor, which agrees with the result obtained by DFTB method.[5] The obtained E_g of ∼3 eV is also bigger than that of DFTB calculation (2.09 eV).

Slab B can be constructed from 1D C_{36} polymers along the *a* or *b* axis (simply called *a* or *b* chain) by extending along the *b* or *a* direction. In fact, we also have calculated 1D *a* and *b* chains using the same SCF−CO method with B3LYP/3-21G and B3LYP/6-31G*. They are semiconductors similar to the results of semiempirical CNDO−CO calculations.[9] These show that the intrinsic semiconductor properties are not altered from 1D chains extending to 2D slabs. It means that the interchain interaction cannot be expected to change these semiconductors to conductors, even the covalent bonds between neighbor chains are formed. Usually, the interchain interaction is a nonbonding interaction and should be weaker in those considered as 1D structures. Therefore, interchain interaction is not enough to change the basic electronic structures of 1D fullerenes.

Crystal orbital analysis shows that the bands near Fermi level are nondegenerate for all five slabs. According to the data listed in Table 2, the top of HOB of slabs A, C, and E are higher than the highest occupied molecular orbital of single C_{36} molecule (−5.61 and −5.15 eV, respectively, for 3-21G and 6-31G*), but lower for slabs B and D. Moreover the bottoms of LUB for all the semiconductor polymers are higher than the lowest unoccupied molecular orbital of C_{36} molecule (−4.58 and −4.05 eV, respectively, for 3-21G and 6-31G*). Although Koopmans' theorem is not valid in DFT calculations, the relative order of frontier orbitals still reflects the relative ability of losing and accepting an electron. Therefore, forming 2D C_{36} slabs would lead to increase of ionization potential except for slabs B and D and reduce the electron affinity. This should be unfavorable to doping of electron donors.

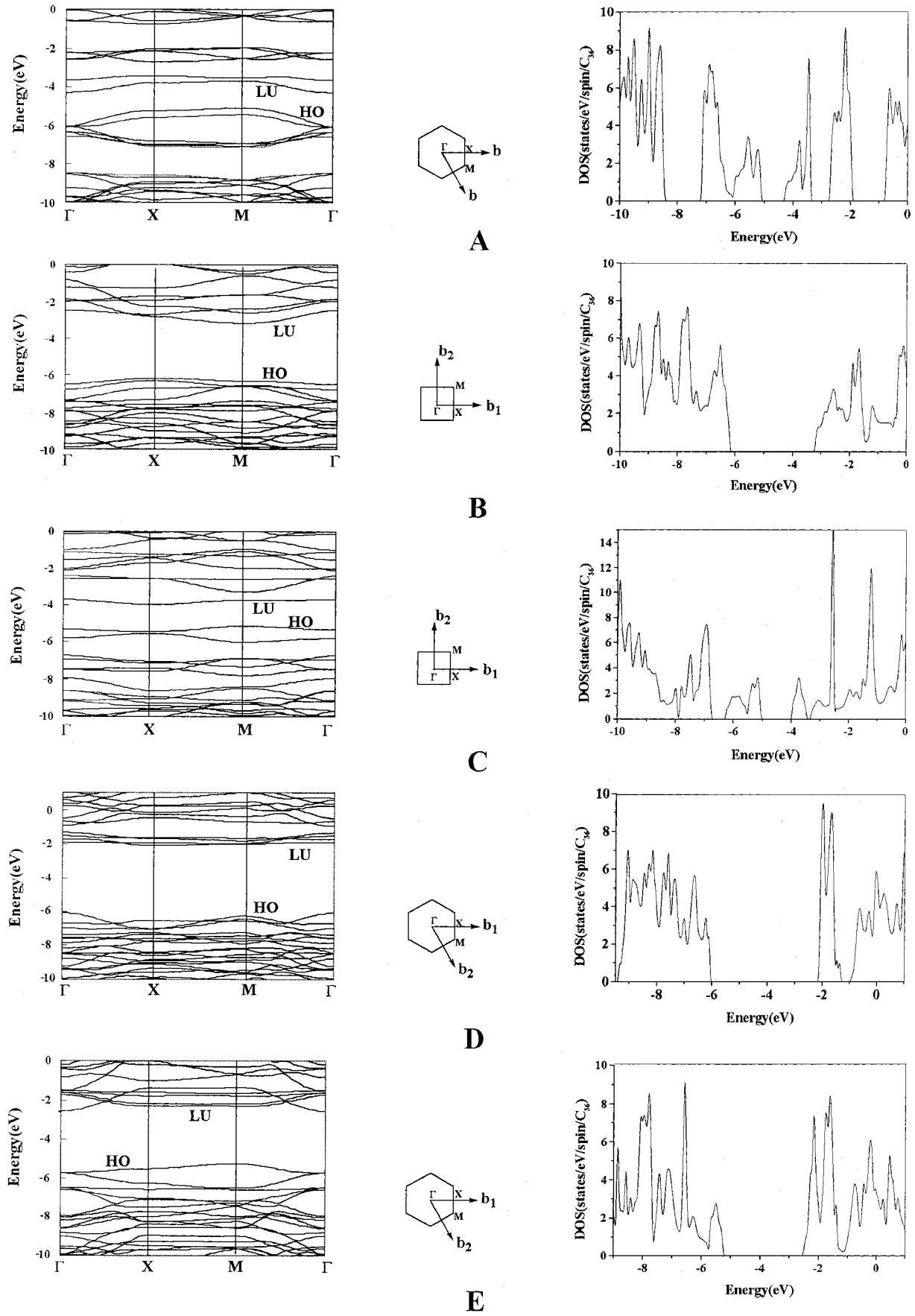

Figure 2. Band structures, Brillouin zones and DOS of neutral C_{36} slabs (calculated with 3-21G).

Now we discuss the corresponding C_{36}^{m-} slabs A−E. Especially, we pay attention to whether the rigid-band picture can be worked in C_{36}^{m-} with increase of *m*. Calculations show that changes of band structures are similar for all five model slabs with both 3-21G and 6-31G*. Therefore, only the 3-21G band structures of anionic slab B are shown in Figure 4. Slab

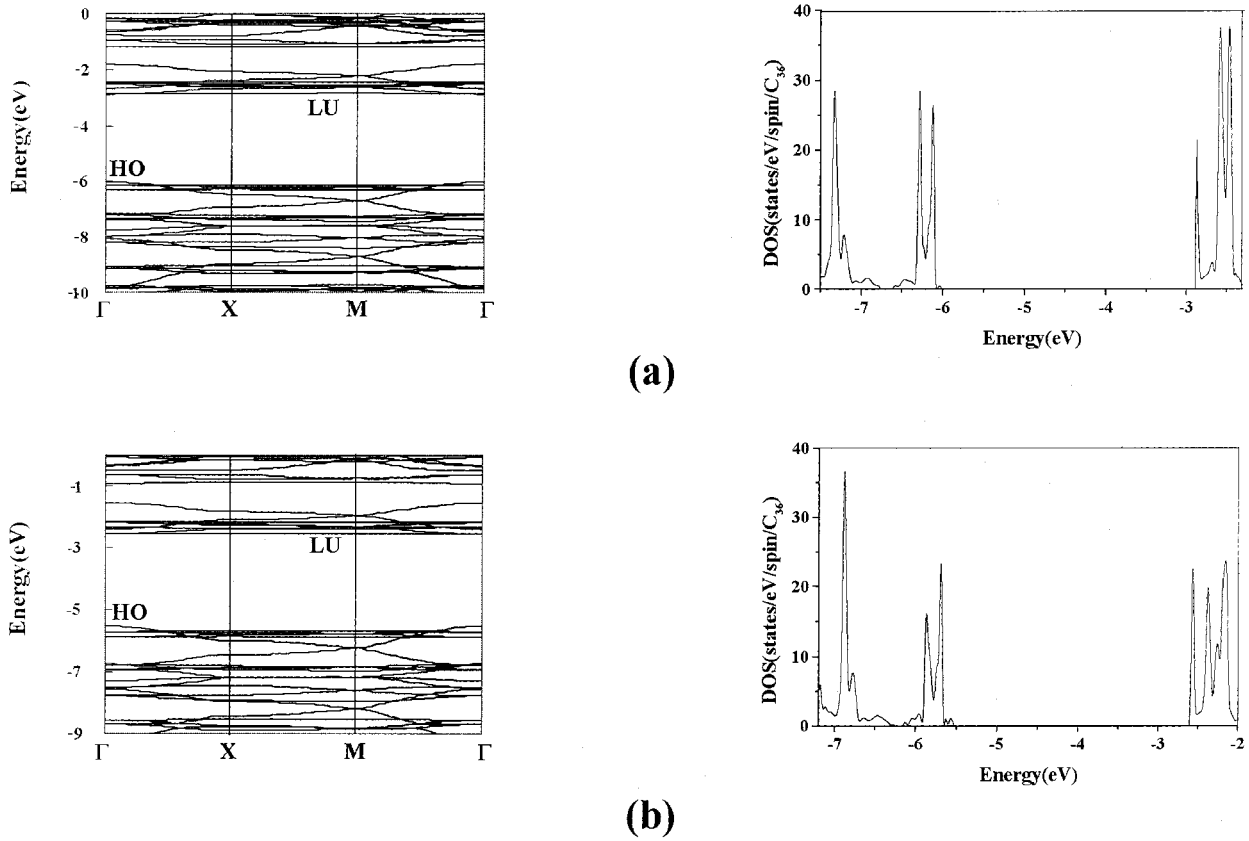

Figure 3. Band structures and DOS of supergraphite slab. (a) 3-21G; (b) 6-31G*.

TABLE 2: Electronic Properties of Slabs A, B, C, D, E, and Supergraphite (in eV)

	E_g		top of HOB		bottom of LUB		HOBW		LUBW	
slab	3-21G	6-31G*	3-21G	6-31G*	3-21G	6-31G*	3-21G	6-31G*	3-21G	6-31G*
A	0.81	0.58	−5.10	−4.12	−4.30	−3.54	0.96	0.99	0.60	0.65
B	3.01	2.94	−6.20	−5.75	−3.19	−2.81	0.32	0.23	0.70	0.54
C	1.19	1.08	−5.17	−4.78	−3.98	−3.70	0.30	0.20	0.25	0.29
D	3.97	3.72	−6.07	−5.65	−2.09	−1.93	0.65	0.67	0.18	0.23
E	2.94	2.69	−5.25	−4.80	−2.31	−2.10	0.48	0.57	0.58	0.56
supergraphite	3.12	2.96	−6.01	−5.54	−2.89	−2.58	0.68	0.69	0.04	0.01

B is selected as an example, because it is the most stable structure.

Compared with the band structures of the neutral slab in Figure 2, the extra electrons fill the unoccupied bands almost in a rigid-band manner, the shape of bands change little. This indicates that the rigid-band theory is valid in 2D C_{36}^{m-} slabs if the geometrical structures are kept unchanged. The plane-wave pseudopotential density functional calculation showed that the original crystal structure had little relaxation in 3D Na_2C_{36} crystal upon introducing the intercalant.[8] The situation should be similar in 2D crystals if the doping atoms are small, especially they can be intercalated in the interspaces between two layers. With the electron filling, slab A shows the alternate changes of conductor and semiconductor with increase of m; slab C becomes semiconductors at $m = 2$, as well as slabs D and E at $m = 4$; the others are kept as conductors for $m = 1-4$. The results are not difficult to understand from Figure 2 with a rigid-band filled picture for A, B, and C. As to slabs D and E, LUB+2 contacts with LUB+3 under the neutral condition. When LUB+2 is filled with electrons, it separates from LUB+3; and slabs D and E, with completely filled LUB+2, become semiconductors. It can also be seen that the levels of energy bands decrease with the increasing of m. The more the electrons added, the lower the whole energy bands become. Therefore the energies of 2D C_{36}^{m-} crystals always decline with m, which is different from the case in a single C_{36} molecule. DFT/6-31G* calculation indicated that C_{36}^{-} is more stable than C_{36}^{2-}.[28]

As mentioned in the previous section, theoretical work indicated that rhombohedral C_{36} fullerenes with D_{6h} symmetry could lead to high T_c due to strong e−p coupling.[2] In the following, we also make a roughly estimation on the superconducting possibility in 2D C_{36} conductors. Our calculations show that the frontier bandwidths are all smaller than 1 eV as shown in Table 2, similar to those of 3D and 1D C_{36} models.[2,9] Therefore 2D C_{36} structures are somewhat similar to molecular type crystals from a view of band structures, though they are built through covalent bonds. Likewise, intramolecular e−p interaction is considered only as the assumption in ref 2.

The e−p interacting coupling constant is expressed as $\lambda = NV_{ep}$, where N is DOS per eV per spin per C_{36} at Fermi level, V_{ep} is the e−p interaction potential. The values of N are in the range of 0.9−9.0 states/eV/spin/C_{36} and listed in Table 3. It can be found that both 3-21G and 6-31G* calculations give almost the same results for slabs A, B, and E. But difference of DOS between these two basis sets cannot be neglected for slabs C and D. Since DOS is concerned with dE/dk, a small discrepancy of band structures may result in larger diversity

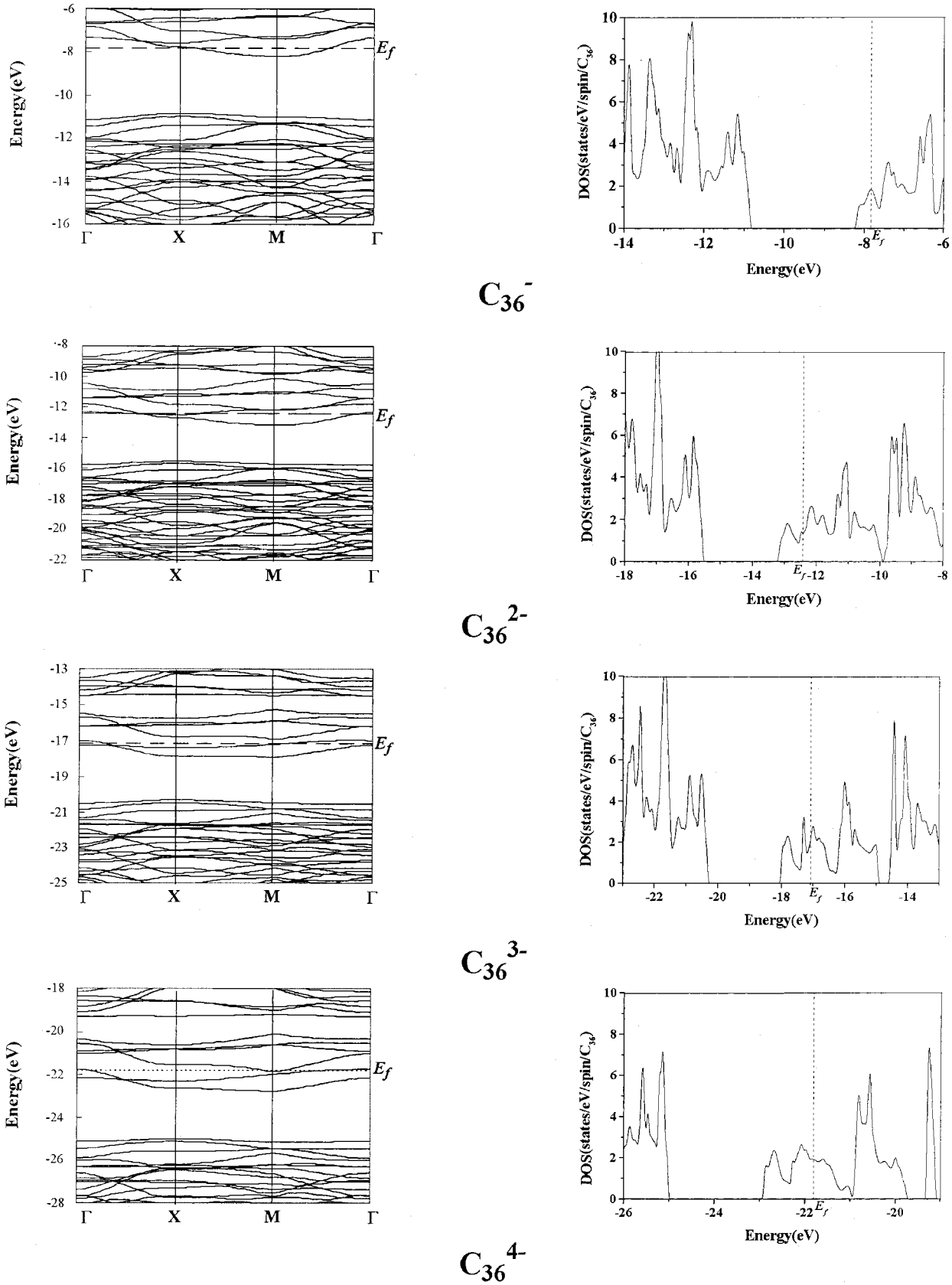

Figure 4. Band structures and DOS of anionic slab *B* (calculated with 3-21G).

for calculation of DOS. According to the e−p interaction estimated for fullerenes,[29] V_{ep} is about 135 ± 11 meV for C_{36} cage. Using the data of N in Table 3 and V_{ep} = 135 meV, coupling constants are of 0.19−0.35 for anionic slab B and 0.47−0.78 for anionic slab E, being not larger than those in alkali metal-doped C_{60} crystals.[30] The tri-anionic slab A has bigger N about 8 states/eV/spin/C_{36}, and gives $\lambda \approx 1$, which may lead to higher T_c. But the five 2D slabs seem impossible to yield T_c (C_{36}) ≈ 6T_c (C_{60}) as predicted for 3D rhombohedral C_{36} solid.[2]

TABLE 3: DOS of the 2D C_{36}^{m-} Slabs at Fermi Level (in states/eV/spin/C_{36})

basis	$m=1$		$m=2$		$m=3$		$m=4$	
set	3-21G	6-31G*	3-21G	6-31G*	3-21G	6-31G*	3-21G	6-31G*
A	1.8	1.3	0	0	7.7	8.3	0	0
B	1.8	2.0	1.4	1.4	2.0	1.9	2.3	2.0
C	2.5	2.1	0	0	9.0	5.0	7.2	5.2
D	8.4	3.2	2.5	1.0	4.5	2.6	0	0
E	3.7	3.5	5.2	5.8	4.5	4.5	0	0

As to the supergraphites, if the rigid-band theory is work, C_{36}^{-} polymer should have larger DOS at Fermi level according to the distribution of DOS shown in Figure 3. Our DFT-321G calculation for the monovalent anionic supergraphite confirms the expectation. The DOS at Fermi level is $N = 20.6$ states/eV/spin/C_{36}, which is in good agreement with that estimated from the distribution of DOS for the neutral supergraphite. Hence a large e−p coupling constant is obtained $\lambda = 2.87$, it may lead to a high T_c. However, most states of contribution to the DOS are from the very narrow band (LUB), usually electron−electron interaction is very strong in a narrow band system, which may greatly suppress superconductivity.

4. Summary

In a brief summary, the energies and band structures of several 2D C_{36} models have been calculated using ab initio B3LYP/DFT method. It is found that the stabilities of 2D C_{36} crystals are concerned with steric hindrance and size of aromatic domains in C_{36} cages. Slab B with D_{2h} symmetry is the most stable structure due to less stack repulsion and bigger aromatic domains among those with a C_{36} cage per unit cell. The supergraphite is even more stable than slab B. All 2D C_{36} models are semiconductors with an E_g of 0.58−3.97 eV. These properties are determined by stacked structures and the linking patterns between neighbor C_{36} cages. Calculations also show that the rigid-band theory is valid in anionic 2D C_{36} crystal slabs under condition of keeping the original geometrical structures of neutral crystals. It predicts that the e−p coupling in metallic polymers with a C_{36} cage per unit cell cannot lead to the superconducting transition temperature much higher than those in alkali metal-doped C_{60} crystals. Although the monovalent anionic supergraphite gives a large e−p coupling constant, the strong electron−electron coupling may greatly suppress superconductivity due to the very narrow partially filled band. Nevertheless, there are most likely more stable structures of C_{36} crystals. Further studies of these solids and quest for superconducting C_{36} are still worth doing.

Acknowledgment. This work was supported by National Natural Science Foundation of China (Grant No. 29873007) and the Major State Basic Research Development Program (Grant No. G2000078100).

References and Notes

(1) Piskoti, C.; Yarger, J.; Zettl, A. *Nature* **1998**, *393*, 771.

(2) Côté, M.; Grossman, J. C.; Cohen, M. L.; Louie, S. G. *Phys. Rev. Lett.* **1998**, *81*, 697.

(3) Heath, J. R. *Nature* **1998**, *393*, 730.

(4) Collins, P. G.; Grossman, J. C.; Côté, M.; Ishigami, M.; Piskoti, C.; Louie, S. G.; Cohen, M. L.; Zettl, A. *Phys. Rev. Lett.* **1999**, *82*, 165.

(5) Fowler, P. W.; Heine, T.; Rogers, K. M.; Sandall, J. P. B.; Seifert, G.; Zerbetto, F. *Chem. Phys. Lett.* **1999**, *300*, 369.

(6) Heine, T.; Fowler, P. W.; Seifert, G. *Solid State Commun.* **1999**, *111*, 19.

(7) Menon, M.; Richter, E. *Phys. Rev. B* **1999**, *60*, 13322.

(8) Grossman, J. C.; Louie, S. G.; Cohen, M. L. *Phys. Rev. B* **1999**, *60*, R6941.

(9) Huang, Y.; Chen, Y.; Liu, R. *J. Phys. Chem. Solids* **2000**, *61*, 1475.

(10) Gal'pern, E. G.; Stankevich, I. V.; Chistyakov, A. L.; Chernozatonskii, L. A. *J. Mol. Graph. Mod.* **2001**, *19*, 189.

(11) Yoshizawa, K.; Tachibana, M.; Yamabe, T. *J. Chem. Phys.* **1999**, *111*, 10088.

(12) Pekker, S.; Jánossy, A.; Mihaly, L.; Chauvet, O.; Carrard, M.; Forró, L. *Science* **1994**, *265*, 1077.

(13) Fowler, P. W.; Heine, T. *J. Chem. Soc., Perkin Trans. 2* **2001**, 487.

(14) Fowler, P. W.; Manolopoulos, D. E. *An Atlas of Fullerenes*; Clarendon: Oxford, 1995.

(15) Grossman, J. C.; Côté, M.; Louie, S. G.; Cohen, M. L. *Chem. Phys. Lett.* **1998**, *284*, 344.

(16) Slanina, Z.; Uhlik, F.; Zhao, X.;Ôsawa, E. *J. Chem. Phys.* **2000**, *113*, 4933.

(17) Frisch, M. J.; Trucks, G. W.; Schlegel, H. B.; Gill, P. M. W.; Johnson, B. G.; Robb, M. A.; Cheeseman, J. R.; Keith, T. A.; Petersson, G. A.; Montgomery, J. A.; Raghavachari, K.; Al-Laham, M. A.; Zakrzewski, V. G.; Ortiz, J. V.; Foresman, J. B.; Cioslowski, J.; Stefanov, B. B.; Nanayakkara, A.; Challacombe, M.; Peng, C. Y.; Ayala, P. Y.; Chen, W.; Wong, M. W.; Andres, J. L.; Replogle, E. S.; Gomperts, R.; Martin, R. L.; Fox, D. J.; Binkley, J. S.; Defrees, D. J.; Baker, J.; Stewart, J. P.; Head-Gordon, M.; Gonzalez, C.; Pople, J. A. *Gaussian 98*; Gaussian, Inc.: Pittsburgh, PA, 1998.

(18) Komaromi, D. S.; Byun, I.; Morokuma, K. S.; Frisch, K. M. *J. THEOCHEM* **1999**, *461*, 1.

(19) Svensson, M.; Humbel, S.; Froese, R. D. J.; Matsubara, T.; Sieber, S.; Morokuma, K. *J. Phys. Chem.* **1996**, *100*, 19357.

(20) Becke, A. D. *Phys. Rev. A* **1988**, *38*, 3098.

(21) Lee, C.; Yang, W.; Parr, R. G. *Phys. Rev. B* **1988**, *37*, 785.

(22) Gordon, M. S.; Binkley, J. S.; Pople, J. A.; Pietro, W. J.; Hehre, W. J. *J. Am. Chem. Soc.* **1982**, *104*, 2797.

(23) Dewar, M. J. S.; Thiel, W. *J. Am. Chem. Soc.* **1977**, *99*, 4899.

(24) Saunders: V. R.; Dovesi, R.; Roetti, C.; Causa, M.; Harrison, N. M.; Orlando, R.; Zicovich-Wilson, C. M. *CRYSTAL98 User's Manual*; University of Torino: Italy, 1998.

(25) Hehre, W. J.; Radom, L.; Schleyer, P. Von R.; Pople, J. A. *Ab Initio Molecular Orbit Theory*; Wiley: New York, 1986.

(26) Kroto, H. W.; Walton, D. R. M. *Chem. Phys. Lett.* **1993**, *214*, 353.

(27) Applequist, D. E.; Depuy, C. H.; Rinehart, K. L. *Introduction to Organic Chemistry*, 3rd ed.; John Wiley & Sons: New York, 1982; Chapter 5.

(28) Ito, A.; Monobe, T.; Yoshii, T.; Tanaka, K. *Chem. Phys. Lett.* **1999**, *315*, 348.

(29) Crespi, V. H. *Phys. Rev. B* **1999**, *60*, 100.

(30) Crespi, V. H.; Hou, J. G.; Xiang, X. D.; Cohen, M. L.; Zettl, A. *Phys. Rev. B* **1992**, *46*, 12064.